

Application of Speed Estimation Techniques for Induction Motor Drives in Electric Traction Industries and vehicles

S. M. Mousavi G¹, A. Dashti²

1. Assistant professor, 2. MSc graduate, Department of Railway Electrification, School of Railway Engineering, Iran University of Science and Technology, Tehran, Iran

* sm_mousavi@iust.ac.ir

Abstract

Induction motors are the most commonly used in the traction industries and electric vehicles, due to their low primary cost, low maintenance costs, and good performance. Speed identification is needed for the induction motor drives. However, using of speed sensors in the induction motor drives is associated with problems such as, extra cost, reduced reliability, added mounting space, etc.. Therefore, many of the recent researches had been dedicated to sensor less induction motor drives. In the induction motor, the rotor speed is estimated using measured stator voltages and currents of the induction motor, as the sensor less drive. The rotor speed for sensor less induction motor drives can be estimated by various techniques, which is designed with respect to required accuracy and sensitivity against induction motor parameter variation. In this paper, comprehensive review of different induction motor speed estimation techniques for traction applications, their special features and advantages is presented.

Keywords: *Sensor less, induction motor drives, speed estimation*

1. Introduction

In the past, dc motors were preferred as the high-performance electrical motor drive in traction applications and other industries. However, the inherent drawbacks of dc motors have caused continual attempts to find out an alternative for dc motors, e.g., heavy weight, large size, and frequent maintenance requirements. Induction motors have many merits like reliability, low cost, low maintenance and simplicity [1-3]. Precise speed and torque control of an induction motor was impossible due to the serious nonlinear behavior and time varying nature of an induction motor drive. However, advances in solid-state power-electronic switching devices, electronic processing, and control design made them a proper choice for high-performance drive applications [4, 5]. Nowadays, induction motors are the most applicable in the traction and vehicular technologies, which usually is controlled with power-electronic switching devices in electric cars/trains [6]. Modern control methods for an induction motor drive can be divided into the two major classes: field oriented control (FOC) and direct torque control (DTC). Moreover, there are two

variants of FOC: direct field oriented control (DFOC) and indirect field oriented control (IFOC). Usually, IFOC is preferred to DFOC, because the natural robustness of an induction motor drive is reduced by flux sensors used in DFOC [7-10]. There are several types for DTC implementation includes: switching table based, direct self-control, space vector modulation, and constant switching frequency. The features of DTC compared to standard FOC can be classified as follows [11-13]:

Estimation of the stator flux vector and torque is required

Coordinate transformation is not required

Separate voltage PWM is not used

There is not any current control loop

Accurate speed information is necessary for an induction motor drive with modern control techniques. Speed identification can be performed by a physical sensor; however, speed estimation is more commonly used. The most important advantages of sensorless induction motor drive include [14-18]:

Transducer cost avoided

Reduced electrical noise

Increased reliability and robustness

Fewer maintenance requirements

Suitable for hostile environments, including temperature

Recently, sensor less induction motor drives has received intensive attention from the researchers and designers. Basic divisions of induction motor speed estimation techniques are shown in Fig. 1, which are generally classified under two categories, as discussed in [11-17]: (i) signal injection based methods and (ii) fundamental model based methods. The signal injection based methods, suffer from large computation time, complexity and limited bandwidth control [19, 20]. They are used at very low speeds, especially at zero speeds as investigated in [14, 21, 22]. The fundamental model based methods are more common because of their simplicity, and associated problems with the motor anisotropies based method like large computation time, complexity and limited bandwidth control [12, 13]. The fundamental model based methods can be classified as open loop speed calculators, Adaptive Flux Observers (AFO), Sliding Mode Observers (SMO), Extended Kalman Filters (EKF), Model Reference Adaptive Systems (MRAS) and Artificial Intelligence (AI) Techniques. In this paper, a review of different speed estimation techniques of sensorless induction motor drives is

presented. In addition, the problems of a sensor less induction motor drive are introduced.

2. Fundamental model based speed estimation methods

In this part, structures of the fundamental model based speed estimation methods are presented. They can be summarized as follows:

2.1 Open loop observer

The rotor fluxes of the induction motor in the stationary reference frame can be written as follows:

$$\frac{d}{dt}\psi_{rd} = \frac{L_r}{L_m} \left(V_{sd} - R_s i_{sd} - \sigma L_s \frac{d}{dt} i_{sd} \right) \tag{4}$$

$$\frac{d}{dt}\psi_{rq} = \frac{L_r}{L_m} \left(V_{sq} - R_s i_{sq} - \sigma L_s \frac{d}{dt} i_{sq} \right) \tag{5}$$

The block diagram of the open loop observer is shown in Fig. 2, which is very simple and has low computational time. However, it suffers from the following problems [12, 16]:

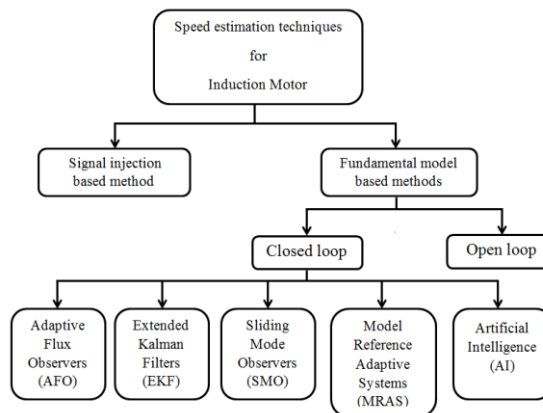


Fig1. Speed estimation techniques of induction motor

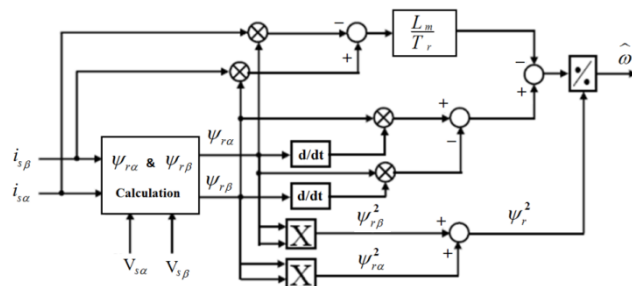


Fig2. Block diagram of open loop observer

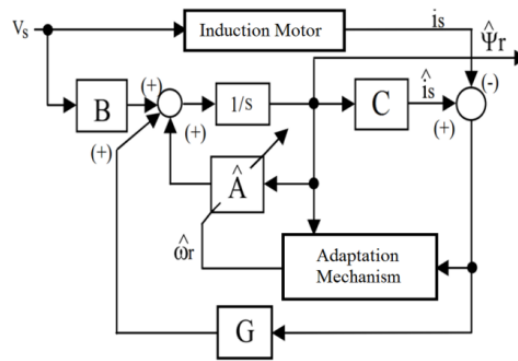


Fig3. Block diagram of the adaptive flux observer

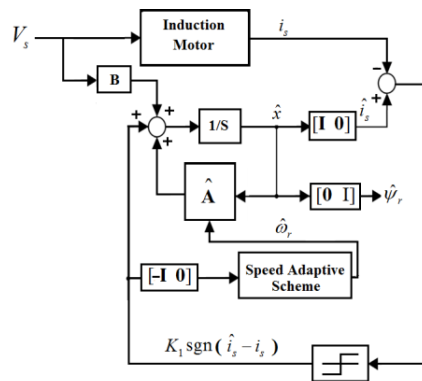


Fig4. Block diagram of the sliding mode observer

$$\frac{d}{dt} \begin{bmatrix} i_{s\alpha} \\ i_{s\beta} \\ \psi_{s\alpha} \\ \psi_{s\beta} \end{bmatrix} = \begin{bmatrix} -a_1 & 0 & a_2 & a_3\omega_r \\ 0 & -a_1 & -a_3\omega_r & a_2 \\ a_4 & 0 & -a_5 & -\omega_r \\ 0 & a_4 & \omega_r & -a_5 \end{bmatrix} \begin{bmatrix} i_{s\alpha} \\ i_{s\beta} \\ \psi_{s\alpha} \\ \psi_{s\beta} \end{bmatrix} + \frac{1}{\sigma L_s} \begin{bmatrix} V_{s\alpha} \\ V_{s\beta} \end{bmatrix} \quad (6)$$

$$\begin{bmatrix} i_{s\alpha} \\ i_{s\beta} \end{bmatrix} = \begin{bmatrix} 1 & 0 & 0 & 0 \\ 0 & 1 & 0 & 0 \end{bmatrix} \begin{bmatrix} i_{s\alpha} \\ i_{s\beta} \\ \psi_{s\alpha} \\ \psi_{s\beta} \end{bmatrix} \quad (7)$$

where

$$\sigma = 1 - \frac{L_m^2}{L_r L_s}, \quad a_1 = \frac{1}{\sigma L_s} \left(R_s + \frac{L_m^2}{L_r \tau_r} \right), \quad a_2 = \frac{1}{\sigma L_s} \left(\frac{L_m}{L_r \tau_r} \right),$$

$$a_3 = \frac{1}{\sigma L_s} \left(\frac{L_m}{L_r} \right), \quad a_4 = \frac{L_m}{\tau_r}, \quad a_5 = \frac{1}{\tau_r}.$$

We can put the Eqn. 6 and Eqn. 7 into the following component form:

$$\frac{d}{dt} x = Ax + Bu \quad (8)$$

$$y = Cx \quad (9)$$

Where x is state vector, u is input vector, y is output vector. The state vector can be estimated by the following equation:

$$\frac{d}{dt} x = Ax + Bu + G(Cx - y) \quad (10)$$

$$A = \begin{bmatrix} -a_1 & 0 & a_2 & a_3\omega_r \\ 0 & -a_1 & -a_3\omega_r & a_2 \\ a_4 & 0 & -a_5 & -\omega_r \\ 0 & a_4 & \omega_r & -a_5 \end{bmatrix} \quad (11)$$

Where, G is the observer gain. The adaptation mechanism is based on Lyapunov theory and the rotor speed is estimated as follows:

$$\omega_r = \left(K_p + \frac{K_i}{s} \right) \left[(\hat{i}_{sd} - i_{sd}) \psi_{rq} - (\hat{i}_{sq} - i_{sq}) \psi_{rd} \right] \quad (12)$$

The accuracy of speed estimation depends on the assignment of the observer gain G and PI gains. Design of the observer gain G and PI gains is performed based on pole placement approach. In order to get stability at all speeds, the observer poles should be proportional to the motor poles. The accuracy of this method is affected by parameter variations, especially at low speeds, because the observer gain G depends on induction motor parameters [12, 25]. Therefore, the robust control is

hired to design the observer gain Get improve the

2.3 Sliding mode observer

The block diagram of the sliding mode observer for speed estimation of induction motor is shown in Fig. 4. The structure of this method is similar to Luenberger observer method[28]and consists of three main parts: an induction motor model, feedback gain and an adaptation mechanism. The induction motor is modeled by Eqn.7 and Eqn. 8. The state vector is estimated by the following equations[29]:

$$\frac{d}{dt} \hat{x} = \hat{A}\hat{x} + Bu + K_1 \operatorname{sgn}(\hat{i}_s - i_s) \tag{13}$$

$$K_1 = k [I, -I]^T$$

Where K_1 is a gain matrix and k is the switching gain. Based on Lyapunov theory, the rotor speed can be estimated as follows:

$$\hat{\omega}_r = -k \int [\operatorname{sgn}(\hat{i}_{s\alpha} - i_{s\alpha}) \hat{\psi}_{r\beta} - \operatorname{sgn}(\hat{i}_{s\beta} - i_{s\beta}) \hat{\psi}_{r\alpha}] dt \tag{14}$$

Using of the sliding mode control in the senseless induction motor drive for speed estimation provides many suitable features, such as good performance against unpredicted dynamics, insensitivity to parameter variations, external disturbance rejection and fast dynamic response. However chattering problem elimination is required for induction motor speed estimator based on sliding mode observer [30-32].

2.4 Extended Kalman Filter

An Extended Kalman Filter (EKF) is a recursive optimum observer, which can be used for the state and parameter estimation of a nonlinear dynamic system[33].The EKF is suitable for the speed estimation of an induction motor.The block diagram

Luenberger observer performance[26, 27]. of the EKF is shown in Fig. 5. The main design steps of the EKF algorithm for induction motor rotor speed estimation are as follows [13, 33, 34]:

- Discretization of the induction machine model
- Determination of the noise and state covariance matrixes
- Implementation of the EKF algorithm

The compact form of the induction motor state space equations is given as follows:

$$\begin{aligned} \frac{dx(t)}{dt} &= Ax(t) + Bu(t) + v(t) \\ y(t) &= Cx(t) + w(t) \end{aligned} \tag{15}$$

Where $x(t) = [i_{ds}^s \ i_{qs}^s \ \psi_{dr}^s \ \psi_{qr}^s \ \omega_r]^T$ is the state vector, $u(t) = [V_{ds}^s \ V_{qs}^s]^T$ is the input vector, $y(t) = [i_{ds}^s \ i_{qs}^s]^T$ is the output vector. $v(t)$ and $w(t)$ are the input noise and output noise respectively. The discrete time form of equation (15) is given below:

$$\begin{aligned} x(k+1) &= A_d x(k) + B_d u(k) + v(k) \\ y(k) &= C_d x(k) + w(k) \end{aligned} \tag{16}$$

After initializing covariance matrices Q, R, P (the system noise matrix, measurement noise matrix, and system state matrix respectively), the state vector $x(k)$ is estimated. The estimation of the state vector $x(k)$ consists of six steps:

Prediction of the state vector

$$\begin{aligned} x_{k+1|k} &= A_d x_{k|k} + B_d u(k) \\ x_{k+1|k} &\square F(k+1, k, x_{k|k}, u(k)) \end{aligned} \tag{17}$$

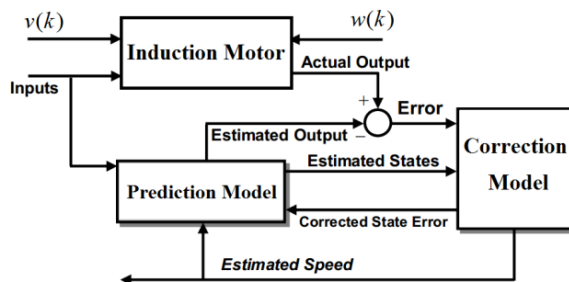


Fig5. block diagram of the EKF

The notation $x_{k+1|k}$ means that it is a predicted value at the (k+1)-the instant and it is based on measurements up to k-the instant, F is Jacobian matrices.

Prediction of the covariance matrix P

$$P_{k+1|k} = MP_{k|k}M^T + Q$$

$$M = \frac{\partial F}{\partial x} \Big|_{x=x_{k|k}} \tag{18}$$

EKF Gain Computation

$$L_k = P_{k|k-1}N^T [NP_{k|k-1}N^T + R]^{-1} \tag{19}$$

Where

$$N = \frac{\partial h}{\partial x} \Big|_{x=x_{k|k-1}}$$

$$h \square C_d x_{k|k+1} = \begin{bmatrix} i_{ds}^s \\ i_{qs}^s \end{bmatrix} \tag{20}$$

State Vector Estimation

$$x_{k|k} = x_{k|k-1} + L_k (y_k - y_k) \tag{21}$$

where

$$y_k = C_d x_{k|k-1} \tag{22}$$

Estimation of the covariance matrix P

$$P_{k|k} = P_{k|k-1} - L_k \frac{\partial h}{\partial x} \Big|_{x=x_{k|k-1}} P_{k|k-1} \tag{23}$$

After all steps executed, set k=k+1 and start from the step 1. The EKF is straightforward and simple; however it suffers from bellow drawbacks [35, 36]:

- Instability due to linearization and erroneous parameters
- Biasedness of its estimates
- Costly calculation of Jacobian matrices
- Lack of analytical methods for model covariance selection.

2.5 Model Reference Adaptive System

Model reference adaptive system (MRAS) based methods are one of the best techniques to estimate rotor speed of induction motor due to their design simplicity and fewer computation requirement compared with other closed-loop model-based methods. As shown in Fig. 6, the basic structure of the MRAS speed estimator consists of a reference model, adjustable model and an adaptation mechanism. Variable x is calculated in the reference model by using measured stator currents and stator voltages. The variable x is estimated in the adjustable model. The adaptive mechanism uses the error (e) between the calculated variable x and the estimated variable

x to generate the estimated speed (ω_r) for the adjustable model. The adaptive mechanism is derived by using Popov's criterion of hyper stability [37]. MRAS based speed estimators developed so far can be divided among four groups:

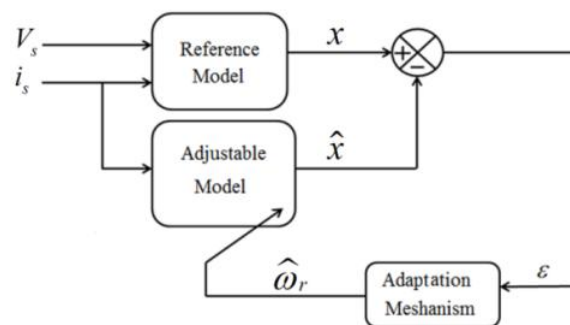


Fig6. General structure of MRAS

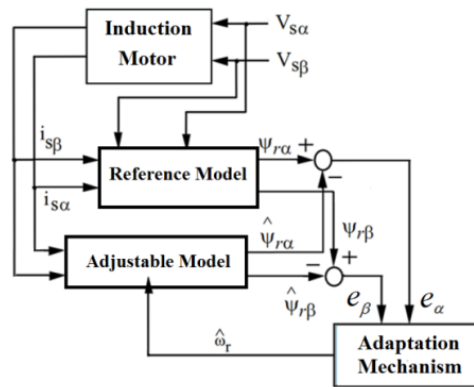


Fig7. Structure of rotor flux based MRAS

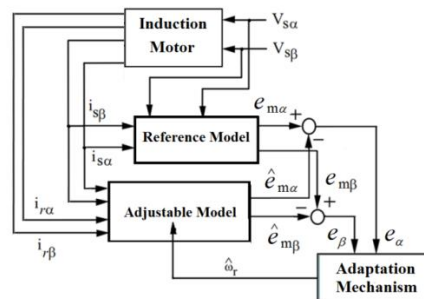


Fig8. structure of back-emf based MRAS

2.5.1 Rotor Flux based MRAS

The rotor flux based MRAS is introduced by Schauder in[37].The structure of this method is shown in Fig. 7.In the rotor flux based MRAS, the rotor flux vector Ψ_r is calculated in the reference model(Eqn. 25 and Eqn. 26).In the adjustable model, the rotor flux vector is estimated (Eqn.27 and Eqn. 28). The error vector (e) is made by the difference between calculated rotor flux vector and estimated rotor fluxvector.The error vector is multiplied to calculated rotor fluxvectorto make speed tuning signal (\mathcal{E}), which is then fed to a PI-type controller, which in turn, outputs the estimated rotor speed (Eqn.31).

$$\Psi_{r\alpha} = \left(\frac{L_r}{L_m}\right) \left[\int (V_{s\alpha} - R_s i_{s\alpha}) dt - \sigma L_s i_{s\alpha} \right] \quad (24)$$

$$\Psi_{r\beta} = \left(\frac{L_r}{L_m}\right) \left[\int (V_{s\beta} - R_s i_{s\beta}) dt - \sigma L_s i_{s\beta} \right] \quad (25)$$

$$\Psi_{r\alpha} = \left(\frac{1}{T_r}\right) \int (L_m i_{s\alpha} - \Psi_{r\alpha} - \omega_r T_r \Psi_{r\beta}) dt \quad (26)$$

$$\Psi_{r\beta} = \left(\frac{1}{T_r}\right) \int (L_m i_{s\beta} - \Psi_{r\beta} - \omega_r T_r \Psi_{r\alpha}) dt \quad (27)$$

$$e_\alpha = \Psi_{r\alpha} - \hat{\Psi}_{r\alpha} \quad (28)$$

$$e_\beta = \Psi_{r\beta} - \hat{\Psi}_{r\beta}$$

$$\mathcal{E} = \Psi_r \otimes e = \Psi_{r\alpha} \Psi_{r\beta} - \Psi_{r\beta} \Psi_{r\alpha} \quad (29)$$

$$\omega_r = \left(K_p + \frac{K_i}{S}\right) \mathcal{E} = \left(K_p + \frac{K_i}{S}\right) (\Psi_{r\alpha} \Psi_{r\beta} - \Psi_{r\beta} \Psi_{r\alpha}) \quad (30)$$

In this method, the stator resistance is appeared in the reference model. The stator resistance varies with temperature, and this affects the stability performance of the speed observer, especially at low speeds. Furthermore, the presence of pure integrators in the reference model leads drift and initial condition problems. To avoid these problems, low-pass filters are used instead of pure integrators; however, they cause serious problems at low speeds and introduce a time-delay[38, 39].

2.5.2 Back-EMF based MRAS

In the back-emf based MRAS, the back-emf vector is produced with the reference model and adjustable model instead of the rotor flux vector[40]. Fig. 8 illustrates structure of the back-emf based MRAS speed estimator. The back-emf vector can be calculated by Eqn.32 and Eqn. 33(as the reference model) or can be estimated by Eqn. 34 and Eqn. 35(as adjustable model). The adaptation mechanism of this method is similar to that of the flux rotor based MRAS. The rotor speed can be estimated by Eqn. 37.

$$e_{m\alpha} = v_{s\alpha} - \left[R_s i_{s\alpha} + \sigma L_s \frac{di_{s\alpha}}{dt} \right] \tag{31}$$

$$e_{m\beta} = v_{s\beta} - \left[R_s i_{s\beta} + \sigma L_s \frac{di_{s\beta}}{dt} \right] \tag{32}$$

$$\hat{e}_{m\alpha} = \frac{-L_m}{L_r} \left[\omega_r (L_m i_{s\beta} + L_r i_{r\beta}) + R_r i_{r\alpha} \right] \tag{33}$$

$$\hat{e}_{m\beta} = \frac{L_m}{L_r} \left[\omega_r (L_m i_{s\alpha} + L_r i_{r\alpha}) - R_r i_{r\beta} \right] \tag{34}$$

$$\varepsilon = e_m \otimes e = \Psi_{r\alpha} \Psi_{r\beta} - \Psi_{r\beta} \Psi_{r\alpha} \tag{35}$$

$$\omega_r = \left(K_p + \frac{K_I}{S} \right) \varepsilon = \left(K_p + \frac{K_I}{S} \right) (\hat{e}_{m\alpha} e_{m\beta} - \hat{e}_{m\beta} e_{m\alpha}) \tag{36}$$

The back-emf based MRAS is dependent upon the variation of stator resistance due to the presence of stator resistance in the reference model. Therefore, accurate sensing of the back-emf is impossible, especially at low speeds. In addition, the presence of derivative operator in the reference model reduces the signal-to-noise ratio considerably at low speeds[12, 13, 41].

2.5.3 Reactive power based MRAS

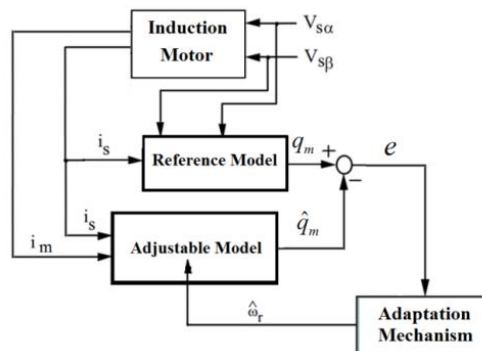


Fig9. structure of air-gap reactive power based MRAS

This scheme can be represented into two different ways, the air-gap reactive power based MRAS and the machine terminal reactive power based MRAS. Fig.9 shows the block diagram of speed estimation using air-gap reactive power based MRAS. In the air-gap reactive power based MRAS, the magnitude of air-gap reactive power is produced with the reference model and adjustable model. The air-gap reactive power can be calculated by Eqn.38 or can be estimated by eqn. 39, so Eqn. 40 and Eqn. 41 are considered as the reference model and the adjustable model, respectively. The rotor speed can be estimated by Eqn. 42, where a PI controller is utilized as the adaptation mechanism[15, 42].

$$\vec{q}_m = \vec{i}_s \otimes \left(\vec{v}_s - \sigma L_s \frac{d\vec{i}_s}{dt} \right) \tag{37}$$

$$\vec{q}_m = L'_m \left((\vec{i}_m \square \vec{i}_s) \omega_r + \frac{1}{T_r} \vec{i}_m \otimes \vec{i}_s \right) \tag{38}$$

$$q_m = |\vec{q}_m| = \left| \vec{i}_s \otimes \left(\vec{v}_s - \sigma L_s \frac{d\vec{i}_s}{dt} \right) \right| \tag{39}$$

$$\hat{q}_m = |\hat{\vec{q}}_m| = \left| L'_m \left((\vec{i}_m \square \vec{i}_s) \hat{\omega}_r + \frac{1}{T_r} \vec{i}_m \otimes \vec{i}_s \right) \right| \tag{40}$$

$$\omega_r = \left(K_p + \frac{K_I}{S} \right) (q_m - \hat{q}_m) \tag{41}$$

The air-gap reactive power based MRAS is completely robust to the stator resistance. However, the reference model is dependent on leakage inductances. In addition, the presence of derivative operator in the reference model reduces the signal to noise ratio, considerably at low speeds[43].

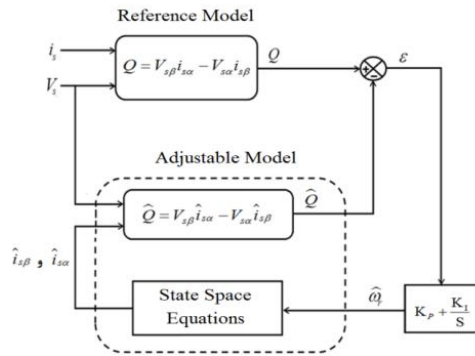


Fig10. structure of machine terminal reactive power based MRAS

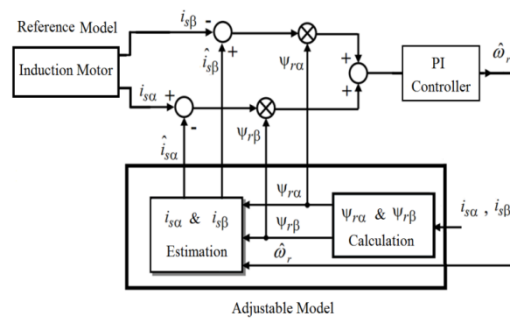


Fig11. structure of stator current based MRAS

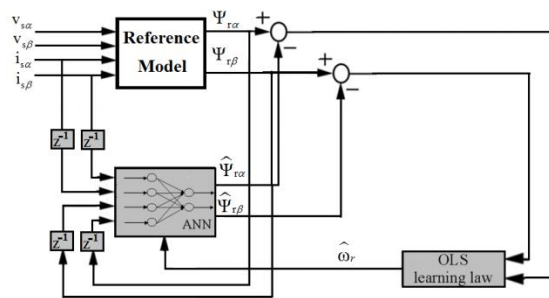


Fig12. ANN rotor flux based MRAS

To eliminate problems of the air-gap reactive power based MRAS, the reactive power is computed at the machine terminal, instead of the air-gap[44]. The structure of the machine terminal reactive power based MRAS is shown in Fig. 10, which Eqn. 43 is utilized in the reference model and Eqn. 44, is utilized in the adjustable model. In the reference model, the measured stator currents are used to calculate the machine terminal reactive power whereas in the adjustable model, estimated stator currents are used to estimate the machine terminal reactive power. The machine state space equations are utilized to estimate the stator currents[16](Eqn. 45).The adaptation mechanism consists of a PI controller where uses

difference between calculated and estimated machine terminal reactive power as input. Therefore, estimated speed can be presented by Eqn. 46.

$$Q = V_{s\beta}i_{s\alpha} - V_{s\alpha}i_{s\beta} \tag{42}$$

$$Q = V_{s\beta}\hat{i}_{s\alpha} - V_{s\alpha}\hat{i}_{s\beta} \tag{43}$$

$$\frac{d}{dt} \begin{bmatrix} \hat{i}_{s\alpha} \\ \hat{i}_{s\beta} \\ \psi_{r\alpha} \\ \psi_{r\beta} \end{bmatrix} = \begin{bmatrix} -a_1 & 0 & a_2 & a_1\omega \\ 0 & -a_1 & -a_2\omega & a_2 \\ L_s & 0 & -\frac{1}{T_r} & -\omega \\ 0 & \frac{L_m}{T_r} & \omega & -\frac{1}{T_r} \end{bmatrix} \begin{bmatrix} \hat{i}_{s\alpha} \\ \hat{i}_{s\beta} \\ \psi_{r\alpha} \\ \psi_{r\beta} \end{bmatrix} + \frac{1}{\delta L_s} \begin{bmatrix} V_{s\alpha} \\ V_{s\beta} \end{bmatrix} \tag{44}$$

$$\omega_r = \left(K_p + \frac{K_I}{S} \right) (Q - Q) \tag{45}$$

2.5.4 Stator Current based MRAS

Fig. 11 shows a block diagram of the stator current based MRAS method, in which, the measured stator currents of the induction motor are used as the reference model, whereas the estimated stator currents of the induction motor are considered as the adjustable model[45]. To estimate the stator currents, the information on the rotor fluxes is required. The rotor fluxes are calculated by using measured stator currents (Eqn. 47). The stator currents are estimated by Eqn. 48. Finally, rotor speed is estimated by Eqn. 49[46].

$$\frac{d}{dt} \begin{bmatrix} \psi_{ra} \\ \psi_{r\beta} \end{bmatrix} = \begin{bmatrix} \frac{L_m}{T_r} & 0 & -\frac{1}{T_r} & -\omega_r \\ 0 & \frac{L_m}{T_r} & \omega_r & -\frac{1}{T_r} \end{bmatrix} \begin{bmatrix} i_{sa} \\ i_{s\beta} \\ \psi_{ra} \\ \psi_{r\beta} \end{bmatrix} \tag{46}$$

$$\frac{d}{dt} \begin{bmatrix} \hat{i}_{sa} \\ \hat{i}_{s\beta} \end{bmatrix} = \begin{bmatrix} -a_1 & 0 & a_2 & a_3 \omega_r \\ 0 & -a_1 & -a_3 \omega_r & a_2 \end{bmatrix} \begin{bmatrix} \hat{i}_{sa} \\ \hat{i}_{s\beta} \\ \psi_{ra} \\ \psi_{r\beta} \end{bmatrix} + \frac{1}{\delta L_s} \begin{bmatrix} V_{sa} \\ V_{s\beta} \end{bmatrix} \tag{47}$$

$$\omega_r = \left(K_p + \frac{K_I}{S} \right) \left[(i_{sa} - \hat{i}_{sa}) \psi_{r\beta} - (i_{s\beta} - \hat{i}_{s\beta}) \psi_{ra} \right] \tag{48}$$

Performance of the stator current based MRAS and the machine terminal reactive power based MRAS are better than other MRAS speed estimator (especially at low speeds) due to absence of induction motor’s parameters and derivative operator in the reference model. The main merits of MRAS method include[15, 43]:

- Simple structure
- Fast convergence
- Robustness
- Small computation time

Demerits include:

- Arduousness of the adaptation mechanism design
- Sensitivity to inaccuracy in the reference model

2.6 Artificial neural network methods

The artificial intelligence (AI) methods are robust to parameter variations, and a nonlinear function can be approximated with any desired degree of accuracy[47]. The induction motor is inherently a nonlinear system and its parameter varies during

operation. Therefore, it is very difficult to estimate the rotor speed with good accuracy for an entire speed range and transient states[12]. For these reasons, the AI methods are used for speed estimation of induction motor. The AI method can take various forms for speed estimation of induction motor such as artificial neural networks (ANN)[48, 49] and fuzzy-neural network (FNN)[50, 51]. The AI methods can estimate the speed independently or use in adaptation mechanism of other methods[52, 53]. For instance, the ANN is used instead both the adjustable model, and the adaptation mechanism of the rotor flux based MRAS method[54], as shown in Fig. 12. In spite of good performance of the AI methods, they have high complexity and slow convergence.

3. Conclusion

In this paper, different speed estimation methods for using in the sensor less induction motor drive and corresponding merits and demerits have been presented. There are two main class of speed estimator for the induction motor, signal injection based method and fundamental model based method. The parameter sensitivity in the signal injection based methods is low; in addition, they perform well at near zero speed. However, they include problems such as, large computation time, limited bandwidth control and computational complexity. The fundamental model based methods are characterized by their simplicity and perform well in the high and medium speed range. At low speeds, they suffer from observability problems. The main sources of inaccuracy in the speed estimation at low speeds include (i) the parasitic components in the measured signals (stator currents and voltages), can affect the accuracy of speed estimation by producing substantial offsets in estimated flux linkage, (ii) The magnitude and phase error in the stator voltages are occurred due to nonlinear properties of PWM inverter, and (iii) parameter variations, especially stator and rotor resistances. To obtain good speed estimation accuracy, estimation of the stator and rotor resistances is necessary. Among fundamental model based methods, SMO has the best behavior. Stator current base MRAS and reactive power based MRAS perform very well; however, their adaptation mechanism design is difficult. Adaptive flux observer has good behavior at high and medium speeds; however, it has considerable inaccuracy at low speeds. As a final comment, when low speed operation is required, signal injection methods are recommended. In a noisy environment, EKF is the best choice since it performs as optimal filtering.

Reference

- [1]. B. K. Bose, "Power electronics and AC drives," *Englewood Cliffs, NJ, Prentice-Hall, 1986, 416 p.*, vol. 1, 1986.
- [2]. A. Consoli, G. Scarcella, and A. Testa, "Slip-frequency detection for indirect field-oriented control drives," *IEEE Trans. Ind. Appl.*, vol. 40, pp. 194-201, 2004.
- [3]. A. Leon and J. Solsona, "On state estimation in electric drives," *Energy Conversion and Management*, vol. 51, pp. 600-605, 2010.
- [4]. J. Faiz and M. B. B. Sharifian, "Different techniques for real time estimation of an induction motor rotor resistance in sensorless direct torque control for electric vehicle," *IEEE Trans. Energy Conv.*, vol. 16, pp. 104-109, 2001.
- [5]. M. Farasat, A. M. Trzynadlowski, and M. S. Fadali, "Efficiency improved sensorless control scheme for electric vehicle induction motors," *IET Elec. Syst. Transportation*, vol. 4, pp. 122-131, 2014.
- [6]. S. M. Mousavi G, A. Tabakhpour Langerudy, E. F. Fuchs, and K. Al-Haddad. "Power Quality Issues in Railway Electrification: A Comprehensive Perspective". *IEEE Trans. Ind. Electron.* 2015. Available: [dx.doi.org/10.1109/TIE.2014.2386794](https://doi.org/10.1109/TIE.2014.2386794)
- [7]. R. Krishnan and A. Bharadwaj, "A review of parameter sensitivity and adaptation in indirect vector controlled induction motor drive systems," *IEEE Trans. Power Electron.*, vol. 6, pp. 695-703, 1991.
- [8]. R. Krishnan, *Electric motor drives: modeling, analysis, and control*: Prentice Hall, 2001.
- [9]. B. Wu, *High-power converters and AC drives*: John Wiley & Sons, 2006.
- [10]. R. Marino, P. Tomei, and C. M. Verrelli, *Induction motor control design*: Springer, 2010.
- [11]. G. S. Buja and M. P. Kazmierkowski, "Direct torque control of PWM inverter-fed AC motors—a survey," *IEEE Trans. Ind. Electron.*, vol. 51, pp. 744-757, 2004.
- [12]. J. W. Finch and D. Giaouris, "Controlled AC electrical drives," *IEEE Trans. Ind. Electron.*, vol. 55, pp. 481-491, 2008.
- [13]. M. S. Zaky, M. M. Khater, S. S. Shokralla, and H. A. Yasin, "Wide-Speed-Range Estimation With Online Parameter Identification Schemes of Sensorless Induction Motor Drives," *IEEE Trans. Ind. Electron.*, vol. 56, pp. 1699-1707, 2009.
- [14]. J. Holtz, "Sensorless control of induction motor drives," *Proc. of the IEEE*, vol. 90, pp. 1359-1394, 2002.
- [15]. P. Brandstetter, M. Kuchar, and D. Vinklerek, "Estimation techniques for sensorless speed control of induction motor drive," in *IEEE Int. Symp. Ind. Electron., 2006*, 2006, pp. 154-159.
- [16]. S. Maiti and C. Chakraborty, "A new instantaneous reactive power based MRAS for sensorless induction motor drive," *Simulation Modelling Practice and Theory*, vol. 18, pp. 1314-1326, 2010.
- [17]. Z. El-Barbary, "Single-to-three phase induction motor sensorless drive system," *Alexandria Engineering Journal*, vol. 51, pp. 77-83, 2012.
- [18]. Z. Xi, "Sensorless Induction Motor Drive Using Indirect Vector Controller and Sliding-Mode Observer for Electric Vehicles," *IEEE Trans. Vehicular Tech.*, vol. 62, pp. 3010-3018, 2013.
- [19]. J.-I. Ha and S.-K. Sul, "Sensorless field-orientation control of an induction machine by high-frequency signal injection," *IEEE Trans. Ind. Appl.*, vol. 35, pp. 45-51, 1999.
- [20]. J. Holtz, "Sensorless control of induction machines—With or without signal injection?," *IEEE Trans. Ind. Electron.*, vol. 53, pp. 7-30, 2006.
- [21]. L. Baghli, I. Al-Rouh, and A. Rezzoug, "Signal analysis and identification for induction motor sensorless control," *Control engineering practice*, vol. 14, pp. 1313-1324, 2006.
- [22]. P. Zhang, Y. Du, T. G. Habetler, and B. u, "Magnetic effects of DC signal injection on induction motors for thermal evaluation of stator windings," *IEEE Trans. Ind. Electron.*, vol. 58, pp. 1479-1489, 2011.
- [23]. J. Maes and J. A. Melkebeek, "Speed-sensorless direct torque control of induction motors using an adaptive flux observer," *IEEE Trans. Ind. Appl.*, vol. 36, pp. 778-785, 2000.
- [24]. M. Boussak and K. Jarray, "A high-performance sensorless indirect stator flux orientation control of induction motor drive," *IEEE Trans. Ind. Electron.*, vol. 53, pp. 41-49, 2006.
- [25]. Z. Zhang, R. Tang, B. Bai, and D. Xie, "Novel direct torque control based on space vector modulation with adaptive stator flux observer for induction motors," *IEEE Trans. Magnetics*, vol. 46, pp. 3133-3136, 2010.
- [26]. F. R. Salmasi, T. A. Najafabadi, and P. Jabehdar-Maralani, "An adaptive flux observer with online estimation of DC-link voltage and rotor resistance for VSI-based induction
- [27]. motors," *IEEE Trans. Power Electron.*, vol. 25, pp. 1310-1319, 2010.
- [28]. M. Jouili, K. Jarray, Y. Koubaa, and M. Boussak, "Luenberger state observer for speed

- [29]. sensorless ISFOC induction motor drives," *Electric Power Systems Research*, vol. 89, pp. 139-147, 2012.
- [30]. S. Rao, M. Buss, and V. Utkin, "Simultaneous state and parameter estimation in induction motors using first-and second-order sliding modes," *IEEE Trans. Ind. Electron.*, vol. 56, pp. 3369-3376, 2009.
- [31]. S. Alireza Davari, D. A. Khaburi, F. Wang, and R. M. Kennel, "Using full order and reduced order observers for robust sensorless predictive torque control of induction motors," *IEEE Trans. Power Electron.*, vol. 27, pp. 3424-3433, 2012.
- [32]. A. Mezouar, M. Fellah, and S. Hadjeri, "Adaptive sliding mode observer for induction motor using two-time-scale approach," *Electric power systems research*, vol. 77, pp. 604-618, 2007.
- [33]. M. Ghanes and G. Zheng, "On sensorless induction motor drives: Sliding-mode observer and output feedback controller," *IEEE Trans. Ind. Electron.*, vol. 56, pp. 3404-3413, 2009.
- [34]. P. T. Doan, T. T. Nguyen, S. K. Jeong, S. J. Oh, and S. B. Kim, "Sensorless Vector Control of AC Induction Motor Using Sliding-Mode Observer," *Int. J. Science and Engineering*, vol. 4, pp. 39-43, 2013.
- [35]. M. Barut, S. Bogosyan, and M. Gokasan, "Speed-sensorless estimation for induction motors using extended Kalman filters," *IEEE Trans. Ind. Electron.*, vol. 54, pp. 272-280, 2007.
- [36]. R. Gunabalan, V. Subbiah, and B. R. Reddy, "Sensorless control of induction motor with extended Kalman filter on TMS320F2812 processor," *measurement*, vol. 500, p. 7, 2009.
- [37]. K. Shi, T. Chan, Y. Wong, and S. Ho, "Speed estimation of an induction motor drive using an optimized extended Kalman filter," *IEEE Trans. Ind. Electron.*, vol. 49, pp. 124-133, 2002.
- [38]. M. Barut, "Bi input-extended Kalman filter based estimation technique for speed-sensorless control of induction motors," *Energy Conversion and Management*, vol. 51, pp. 2032-2040, 2010.
- [39]. C. Schauder, "Adaptive speed identification for vector control of induction motors without rotational transducers," *IEEE Trans. Ind. Appl.*, vol. 28, pp. 1054-1061, 1992.
- [40]. B. Karanayil, M. F. Rahman, and C. Grantham, "An implementation of a programmable cascaded low-pass filter for a rotor flux synthesizer for an induction motor drive," *IEEE Trans. Power Electron.*, vol. 19, pp. 257-263, 2004.
- [41]. E. D. Mitronikas and A. N. Safacas, "An improved sensorless vector-control method for an induction motor drive," *IEEE Trans. Ind. Electron.*, vol. 52, pp. 1660-1668, 2005.
- [42]. M. N. Marwali and A. Keyhani, "A comparative study of rotor flux based MRAS and back EMF based MRAS speed estimators for speed sensorless vector control of induction machines," in *IEEE Conf. Ind. Appl., 1997.*, 1997, pp. 160-166.
- [43]. M. Rashed and A. F. Stronach, "A stable back-EMF MRAS-based sensorless low-speed induction motor drive insensitive to stator resistance variation," *IEE Proc. Elec. Power Appl.*, vol. 151, pp. 685-693, 2004.
- [44]. F.-Z. Peng, T. Fukao, and J.-S. Lai, "Low-speed performance of robust speed identification using instantaneous reactive power for tacholeless vector control of induction motors," in *IEEE Conf. Ind. Electron. Society, 1994*, 1994, pp. 509-514.
- [45]. A. Ravi Teja, C. Chakraborty, S. Maiti, and Y. Hori, "A new model reference adaptive controller for four quadrant vector controlled induction motor drives," *IEEE Trans. Ind. Electron.*, vol. 59, pp. 3757-3767, 2012.
- [46]. C.-M. Ta, T. Uchida, and Y. Hori, "MRAS-based speed sensorless control for induction motor drives using instantaneous reactive power," in *IEEE Conf. Ind. Electron. Society, 2001.*, 2001, pp. 1417-1422.
- [47]. C.-W. Park and W.-H. Kwon, "Simple and robust speed sensorless vector control of induction motor using stator current based MRAC," *Electric Power Systems Research*, vol. 71, pp. 257-266, 2004.
- [48]. T. Orłowska-Kowalska and M. Dybkowski, "Stator-current-based MRAS estimator for a wide range speed-sensorless induction-motor drive," *IEEE Trans. Ind. Electron.*, vol. 57, pp. 1296-1308, 2010.
- [49]. S. M. Gadoue, D. Giaouris, and J. W. Finch, "Sensorless control of induction motor drives at very low and zero speeds using neural network flux observers," *IEEE Trans. Ind. Electron.*, vol. 56, pp. 3029-3039, 2009.
- [50]. M. Cirrincione, M. Pucci, G. Cirrincione, and G.-A. Capolino, "Sensorless control of induction machines by a new neural algorithm: The TLS EXIN neuron," *IEEE Trans. Ind. Electron.*, vol. 54, pp. 127-149, 2007.
- [51]. S. Maiti, V. Verma, C. Chakraborty, and Y. Hori, "An adaptive speed sensorless induction

-
- motor drive with artificial neural network for stability enhancement," *IEEE Trans. Ind. Inform.*, vol. 8, pp. 757-766, 2012.
- [52]. Y. Oguz and M. Dede, "Speed estimation of vector controlled squirrel cage asynchronous motor with artificial neural networks," *Energy Conversion and Management*, vol. 52, pp. 675-686, 2011.
- [53]. F. Lima, W. Kaiser, I. Nunes da Silva, and A. A. de Oliveira, "Speed Neuro-fuzzy Estimator Applied To Sensorless Induction Motor Control," *Latin America Transactions, IEEE*, vol. 10, pp. 2065-2073, 2012.
- [54]. M. Cirrincione and M. Pucci, "Sensorless direct torque control of an induction motor by a TLS-based MRAS observer with adaptive integration," *Automatica*, vol. 41, pp. 1843-1854, 2005.
- [55]. T. Orłowska-Kowalska, M. Dybkowski, and K. Szabat, "Adaptive sliding-mode neuro-fuzzy control of the two-mass induction motor drive without mechanical sensors," *IEEE Trans. Ind. Electron.*, vol. 57, pp. 553-564, 2010.
- [56]. M. Zaky, M. Khater, H. Yasin, and S. Shokralla, "Very low speed and zero speed estimations of sensorless induction motor drives," *Electric Power Systems Research*, vol. 80, pp. 143-151, 2010.